Platinum-Induced Ubiquitination of Phosphorylated H2AX by RING1A Is Mediated by Replication Protein A in Ovarian Cancer

Shruthi Sriramkumar[1], Timothy D. Matthews[1], Ahmed H. Ghobashi[2], Samuel A. Miller[2], Pamela S. VanderVere-Carozza[3], Katherine S. Pawelczak[4], Kenneth P. Nephew[1,5,6], John J. Turchi[3,5], and Heather M. O'Hagan[1,5,7]

ABSTRACT

Platinum resistance is a common occurrence in high-grade serous ovarian cancer and a major cause of ovarian cancer deaths. Platinum agents form DNA cross-links, which activate nucleotide excision repair (NER), Fanconi anemia, and homologous recombination repair (HRR) pathways. Chromatin modifications occur in the vicinity of DNA damage and play an integral role in the DNA damage response (DDR). Chromatin modifiers, including polycomb repressive complex 1 (PRC1) members, and chromatin structure are frequently dysregulated in ovarian cancer and can potentially contribute to platinum resistance. However, the role of chromatin modifiers in the repair of platinum DNA damage in ovarian cancer is not well understood. We demonstrate that the PRC1 complex member RING1A mediates monoubiquitination of lysine 119 of phosphorylated H2AX (γH2AXub1) at sites of platinum DNA damage in ovarian cancer cells. After platinum treatment, our results reveal that NER and HRR both contribute to RING1A localization and γH2AX monoubiquitination. Importantly, replication protein A, involved in both NER and HRR, mediates RING1A localization to sites of damage. Furthermore, RING1A deficiency impairs the activation of the G_2–M DNA damage checkpoint, reduces the ability of ovarian cancer cells to repair platinum DNA damage, and increases sensitivity to platinum.

Implications: Elucidating the role of RING1A in the DDR to platinum agents will allow for the identification of therapeutic targets to improve the response of ovarian cancer to standard chemotherapy regimens.

Introduction

Ovarian cancer is the most lethal gynecologic malignancy and fifth leading cause of death among women. Without the availability of adequate screening methods for early detection, the majority of patients are diagnosed with advanced stage disease (1). The standard of care for treatment of patients with ovarian cancer with advanced disease is surgical debulking followed by platinum-taxane–based chemotherapy (2). High-grade serous ovarian cancer (HGSOC), the most common ovarian cancer histologic type, initially responds to platinum-based therapy (3). However, up to 75% of responding patients relapse and eventually develop platinum-resistant disease. The survival rates of HGSOC have remained essentially unchanged for decades (3). Several mechanisms contribute to the development of platinum resistance, including increased drug efflux, decreased drug uptake, increased detoxification, increased DNA repair, and reduced apoptotic response (4). Epigenetic mechanisms like histone modifications and promoter DNA methylation have also been associated with platinum resistance. Furthermore, dysregulation of chromatin modifiers in cancer leads to an altered DNA damage response (DDR) to chemotherapy agents through altered expression of genes involved in the DDR and altered repair of DNA lesions (5).

Platinum agents—cisplatin and carboplatin—used for treatment of patients with ovarian cancer are DNA-damaging agents. The cytotoxic activity of these agents is due to their ability to cross-link guanines. Cisplatin reacts with N7 positions of two guanines in the DNA forming intrastrand and interstrand cross-links (ICL; ref. 6). Intrastrand adducts, the bulk of cross-links/adducts formed by cisplatin, are repaired by the nucleotide excision repair (NER) pathway (7). Platinum ICLs are repaired by the Fanconi anemia (FA) and homologous recombination repair (HRR) pathways that result in activation of ataxia telangiectasia mutated (ATM) by autophosphorylation at S1981 (pATM; refs. 8, 9). Replication protein A (RPA)–coated single-strand DNA (ssDNA) is a common structure formed during both NER and ICL repair that facilitates downstream DDR (10). ATM and ATR, which are activated by persistent RPA-coated ssDNA, phosphorylate and activate downstream substrates including the histone variant H2AX.

Chromatin modifications occur in the vicinity of DNA damage, to promote signaling and repair of the damage by facilitating access to the DNA repair machinery (11). Cross-talk between DNA repair and chromatin has been explained by the "access, repair and restore" model in which the local chromatin around a site of DNA damage is modified to provide access to repair proteins, followed by repair of the damage

[1]Cell, Molecular and Cancer Biology Graduate Program and Medical Sciences Program, Indiana University School of Medicine, Bloomington, Indiana. [2]Genome, Cell and Developmental Biology, Department of Biology, Indiana University Bloomington, Bloomington, Indiana. [3]Department of Medicine and Department of Biochemistry and Molecular Biology, Indiana University School of Medicine, Indianapolis, Indiana. [4]NERx Biosciences, Indianapolis, Indiana. [5]Indiana University Melvin and Bren Simon Comprehensive Cancer Center, Indianapolis, Indiana. [6]Department of Anatomy, Cell Biology and Physiology; Department of Obstetrics and Gynecology, Indiana University School of Medicine, Indianapolis, Indiana. [7]Department of Medical and Molecular Genetics, Indiana University School of Medicine, Indianapolis, Indiana.

Note: Supplementary data for this article are available at Molecular Cancer Research Online (http://mcr.aacrjournals.org/).

Corresponding Author: Heather M. O'Hagan, Indiana University School of Medicine Bloomington, 1001 East 3rd Street, Bloomington, IN 47405. Phone: 812-855-3035; Fax: 812-855-4436; E-mail: hmohagan@indiana.edu

Mol Cancer Res 2020;18:1699–710

doi: 10.1158/1541-7786.MCR-20-0396

and ultimately restoration of the chromatin to its original state (11). One such chromatin modification at sites of DNA damage is histone ubiquitination, including the monoubiquitination of lysine 119 of H2A/H2AX (H2A/H2AX K119ub1). RING domain-containing polycomb repressive complex 1 (PRC1) members RING1A/B in complex with BMI1 possess E3 ligase activity essential for adding the monoubiquitination mark on H2A/H2AX (12). BMI1 and RING1B localize to sites of IR and enzyme-induced double strand breaks (DSB) and monoubiquitinate H2A/H2AX K119 (13–15). H2A/H2AX monoubiquitination also occurs in response to UV-induced DNA damage, facilitating recruitment of downstream repair proteins and repair activity (16, 17). However, the role of chromatin modifiers and histone modifications in platinum DNA damage in ovarian cancer remains poorly described. With increased repair of platinum adducts and altered DDR being common causes of platinum resistance, it is essential to understand histone modifications occurring at sites of platinum-induced DNA damage.

Here, we demonstrate that RING1A, a member of the PRC1 complex, localizes to sites of platinum DNA damage and monoubiquitinates phosphorylated H2AX (γH2AX). We further show that both the global genome (GG)-NER and HRR pathways converge on γH2AXub1 and contribute to RING1A localization to the damage sites. Inhibition of the DNA binding of RPA decreases localization of RING1A to sites of cisplatin DNA damage. Furthermore, RING1A deficiency results in diminished activation of the G_2–M DNA damage checkpoint, reduced repair of DNA damage, and decreased cell viability after cisplatin treatment. This is the first report of a role for RING1A in the platinum DDR in ovarian cancer. Elucidating the role of RING1A in the DDR to platinum agents will allow for the identification of therapeutic targets to improve the response of ovarian cancer to standard chemotherapy regimens.

Materials and Methods

Cell culture

Cell lines used in the study were maintained at 37°C and 5% CO_2. HGSOC cells—OVCAR5 and Kuramochi—were generously provided by Dr. Kenneth P. Nephew who had the lines authenticated by the ATCC in 2018. OVCAR5 cells were cultured in DMEM 1X (Corning, # MT10013CV) with 10% FBS (Corning, #16000044), and Kuramochi cells were cultured in RPMI 1640 (Gibco, #MT10040CV) with 10% FBS without antibiotics as we have described previously (18). 293T cells obtained from the ATCC were cultured in DMEM 1X with 10% FBS without antibiotics. All the cell lines used in the study were tested for mycoplasma using the Universal mycoplasma detection kit (ATCC, 30-1012K) on October 10, 2019. Cell lines used in all the experiments in the study were passaged for fewer than 15 passages. Note that 154 mmol/L NaCl (Macron Fine Chemicals #7581-12) solution in water was used to make the 1.67 mmol/L stock solution of cisplatin (Millipore Sigma, #232120). Stock solutions of carboplatin at 20 mmol/L (Millipore Sigma, #216100) were made in water. Stock solutions of PRT4165 BMI1-RING1A E3 ligase inhibitor at 10.63 mmol/L (Millipore Sigma, #203630) were made in DMSO. For experiments using this inhibitor, an equivalent amount of DMSO or inhibitor was added along with cisplatin and incubated for the 8 hours at 37°C in 5% CO_2. Cells were pretreated with DMSO or ATM inhibitor KU-55933 (Sigma Aldrich, #SML1109) for 1 hour prior to cisplatin or carboplatin treatment. ATM inhibitor stock solutions were 10 mmol/L in DMSO. Rad51 inhibitor B02 (Millipore Sigma, #553525) stock solutions (50 mmol/L) were made in DMSO and pretreated for 2 hours prior to cisplatin treatment. Stock solutions of RPA inhibitor (RPAi) NERx329 (5 mmol/L) were made in DMSO. All the treatment doses and time points are specified in figure legends.

Generation of stable knockdown lines using viral shRNAs

For knockdown of RING1A (Sigma, SHCLNG-NM_002931, TRCN0000021989, TRCN0000021990), BMI1 (Sigma, SHCLNG-NM_005180, TRCN0000020156, TRCN0000020157), XPC (Sigma, SHCLNG-NM_004628, TRCN0000083119), XPA (Sigma, SHCLNG-NM_000380, TRCN0000083196), CSB (Sigma, SHCLNG-NM_000124, TRCN0000436471), and empty vector (EV) TRC2 (Sigma, SHC201), lentiviral shRNA knockdown protocol from The RNAi Consortium Broad Institute was used. Briefly, 4×10^5 293T cells were plated on day 1 in DMEM 1X containing 10% FBS. On day 2, cells were transfected with shRNA of interest, EV control, and packaging plasmids. Following transfection, 293T cells were incubated at 37°C and 5% CO_2. On day 3, 16 to 18 hours after transfection, media in the transfected flasks were replaced with fresh DMEM containing 10% FBS. Approximately 24 hours later, media containing lentiviral particles were collected, and fresh DMEM + 10% FBS was added. The added media were collected 24 hours later and pooled with media harvested on day 4. This media with lentiviral particles harvested on day 4 and day 5 were filtered using 0.45 μm filter and concentrated using Spin-X concentrator (Corning, #431490).

Antibodies

For Western blot of endogenous proteins, anti-γH2AX [Cell Signaling Technology (CST), #9718, 1:1,000], anti–Actin B (CST, #4970, 1:1,000), anti–p-ATM S1981 (CST, #13050, 1:1,000), anti-total ATM (CST, #2873, 1:1,000), anti-total H2AX (CST, #2595, 1:1,000), anti-RING1A (CST, #13069, 1:1,000), anti-RING1B [Santa Cruz Biotechnology (SC), sc-101109, 1:1,000], anti-H2AK119ub1 (CST, #8240,1:1,000), anti-XPC (SC, sc-74410, 1:1,000), anti-lamin B (SC, sc-6216, 1:1,000; SC, sc-374015, 1:1,000), anti-XPA (SC, sc-28353, 1:1,000), anti-pRPA32 S33 (Bethyl Laboratories, A300-246A-M, 1:1,000), anti-RPA32 (CST, #2208,1:1,000), anti–phospho-Chk1 S345 (CST, #2348, 1:1,000), and anti-total Chk1 (CST, #2360, 1:1,000) antibodies were used. For immunofluorescence, anti-γH2AX (CST, #9718, 1:100), anti-RING1A (Abcam, ab175149, 1:100), anti-RPA32 (CST, #2208, 1:100), anti-Rad51 (Novus biological, NB100-148, 1:100), anti-H2AK119ub1 (Millipore Sigma, 05-678,1:100), and secondary Alexa Conjugate (CST, rat #4416, 1:1,000, mouse #8890, 1:500, rabbit #4412, 1:1,000 and, rabbit #8889,1:500) antibodies were used.

Immunofluorescence with pre-extraction

OVCAR5 cells (2×10^5) were cultured on coverslips in a 6-well plate and incubated at 37°C for 48 hours. After 48 hours, cells were either untreated or treated with cisplatin for 8 hours. For all ATM inhibitor experiments, OVCAR5 cells were not pretreated (Mock), pretreated with DMSO or 15 μmol/L ATM inhibitor (ATMi) for 1 hour, and then untreated (U) or treated with 12 μmol/L cisplatin for 8 hours. For all Rad51 and RPAi experiments, cells were not pretreated (Mock) or pretreated with DMSO or 50 μmol/L B02 (Rad51 inhibitor) or 8 μmol/L NERx329 (RPAi) for 2 hours, respectively and then untreated (U) or treated with 12 μmol/L cisplatin (T) for 8 hours. This was followed by pre-extraction using [0.5% Triton X-100 in 10 mmol/L HEPES (pH 7.4), 2 mmol/L $MgCl_2$, 100 mmol/L KCl, 1 mmol/L EDTA] and then fixed with 4% paraformaldehyde in PBS. Post fixation, cells were permeabilized using 0.5% Triton-X in PBS, blocked with 1% BSA in PBST (PBS + 0.1% Tween-20), incubated with appropriate primary antibodies as indicated, and incubated with

appropriate Alexa Fluor–conjugated secondary antibodies. Coverslips were mounted using prolong gold antifade with DAPI (CST, #8961).

Imaging and quantification

Images for all immunofluorescence experiments (except Supplementary Fig. S1H) were acquired using the Leica SP8 scanning confocal system with the DMi8-inverted microscope. Leica LASX software (Leica Microsystems) was used for image acquisition. All the images were taken using 63X, 1.4NA oil immersion objective at room temperature. Images in Supplementary Fig. S1H were obtained using Nikon NiE upright microscope with Hamamatsu Orca-Flash 2.8 sCMos high-resolution camera. Following image acquisition, images were processed using Image J (National Institutes of Health, Bethesda, MD). For quantifying the percentage of cells with colocalization, at least 100 cells were scored. Each experiment was performed in three biological replicates. Colocalization was also confirmed using RGB profiler plugin on ImageJ as described previously (19).

RNA isolation and quantitative reverse transcription PCR

RNA extraction was performed using the RNAeasy mini kit (Qiagen, 74104). cDNA was synthesized using Maxima first strand cDNA synthesis kit for quantitative reverse transcription PCR (RT-qPCR; Thermo, MA K1642). FastStart Essential DNA green master (Roche, 06402712001) and *CSB* primers were used to amplify the cDNA. RT-qPCR primer sequences for *CSB* were *CSB*, forward, CTATGGTTGAGCTGAGGGCG and *CSB*, Reverse, GGGGATTCCCTCATTTGGCA.

Chromatin extraction

Note that 3×10^6 cells were cultured in 150 mm plates for approximately 48 hours. After UV treatment (see figure legend), cell pellets were used to perform nuclear extraction using CEBN [10 mmol/L HEPES, pH 7.8, 10 mmol/L KCl, 1.5 mmol/L $MgCl_2$, 0.34 mol/L sucrose, 10% glycerol, 0.2% NP-40, 1X protease inhibitor cocktail (Sigma, P5726), 1X phosphatase inhibitor (Thermo, 88266), and N-ethylmaleimide (Acros organics, 128-53-0)] and then washed with CEB buffer (CEBN buffer without NP-40) containing all the inhibitors. To extract the soluble nuclear fraction, after washing the cell pellets with CEBN buffer, they were resuspended in soluble nuclear buffer (2 mmol/L EDTA, 2 mmol/L EGTA, all inhibitors) and rotated at 4°C for 30 minutes. The remaining cell pellet, i.e., the total chromatin fraction, was lysed using 4% SDS and analyzed by Western blot.

The Cancer Genome Atlas analysis

Datasets of patients with ovarian cancer were compared with normal tissue using The Cancer Genome Atlas (TCGA) TARGET GTEx dataset, accessed using Xenabrowser. Statistical significance was determined by pairwise comparisons using t-test with pooled standard deviations. *P* values were adjusted for FDRs using Benjamini and Hochberg method.

Cell viability assay

Note that 2×10^3 OVCAR5 EV or RING1A shRNA1/2 cells were cultured in 96-well plates for 24 hours. Cells were then treated with 6 μmol/L cisplatin for 3 hours. After treatment, cells were washed with PBS and allowed to recover for the indicated time points in platinum-free media. Cell viability was assessed using the CellTiter-glo Luminescent Cell Viability Assay (Promega, #G7572). Luminescence was detected using SYNERGY H1 microplate reader (Biotek) and Gen 5 software (v 2.09). The experiment was done in 6 technical replicates for each condition at each time point and 3 biological replicates. All luminescence readings were normalized to respective untreated.

Statistical analysis

Percentage of cells with colocalization, relative densitometry, and RT-qPCR data (presented as mean ± SEM) were evaluated by using the Student *t* test in Graphpad prism and excel.

Results

RING1A contributes to platinum-induced monoubiquitination of γH2AX

As HGSOC is the most common ovarian cancer histologic type and most patients are treated with DNA-damaging platinum agents (6), we utilized HGSOC cell lines as a model system to understand the role of chromatin modifiers in the DDR to platinum agents. We first determined the time point at which cisplatin induces H2AX phosphorylation in ovarian cancer cells. γH2AX at S139 is a well-established marker of DNA breaks, including those that arise during the processing of platinum adducts by different repair pathways (20). Treatment of OVCAR5 cells with the IC_{50} dose of cisplatin caused a time-dependent increase in γH2AX (**Fig. 1A**). Blotting for γH2AX with the same antibody previously used to also detect monoubiquitinated γH2AX (γH2AXub1) in response to DSB-inducing agents (21) resulted in a band approximately 8 kD higher than γH2AX. γH2AXub1 was first detected at the 8-hour time point and increased at the 16-hour time point when γH2AX levels were highest (**Fig. 1A**). Cisplatin treatment also induced γH2AXub1 in HGSOC Kuramochi cells at 8- and 16-hour time points (Supplementary Fig. S1A). In addition, treatment of OVCAR5 cells with the IC_{50} dose of carboplatin also induced γH2AXub1 after 16 and 24 hours (Supplementary Fig. S1B). The increased time for detection of γH2AXub1 is in accordance with the finding that formation of DNA adducts by carboplatin was delayed compared with cisplatin due to differences in their aquation rates (22).

High expressions of BMI1, RING1A, and RING1B in recurrent ovarian tumors compared with primary tumors at presentation have been reported (23), and PRC1 members have been implicated in the repair of certain lesions. However, as the role of PRC1 complex members in the DDR to platinum agents in ovarian cancer is not well understood, we first examined the expression of PRC1 members in TCGA ovarian cancer patient data. Expression of BMI1 and RING1B was higher in primary ovarian tumors compared with normal ovarian tissue (Supplementary Fig. S1C). RING1A expression was higher than BMI1 or RING1B in normal ovarian tissue, but expression of RING1A in normal compared with primary tumor samples was not different (Supplementary Fig. S1C). Based on these observations, we hypothesized that BMI1 and RING1A/B contribute to platinum-induced γH2AXub1. To determine which of these PRC1 members contributed to platinum-induced ubiquitination, we independently knocked down BMI1, RING1A, or RING1B. BMI1 or RING1B KD had no effect on cisplatin-induced γH2AXub1 (Supplementary Fig. S1D and S1E). However, RING1A KD followed by cisplatin treatment reduced cisplatin-induced γH2AXub1 compared with an EV control (**Fig. 1B**). The RING1A shRNAs had different effects on γH2AX levels. No change in γH2AX was observed after RING1A KD with shRNA1compared with a significant increase in γH2AX with shRNA2 (**Fig. 1B**), suggesting that the decrease in cisplatin-induced γH2AXub1 observed with RING1A KD was not simply due to reduction in γH2AX levels. Comparison of ratio of γH2AXub1 to γH2AX in EV and RING1A KD cells also demonstrated that there is a significant

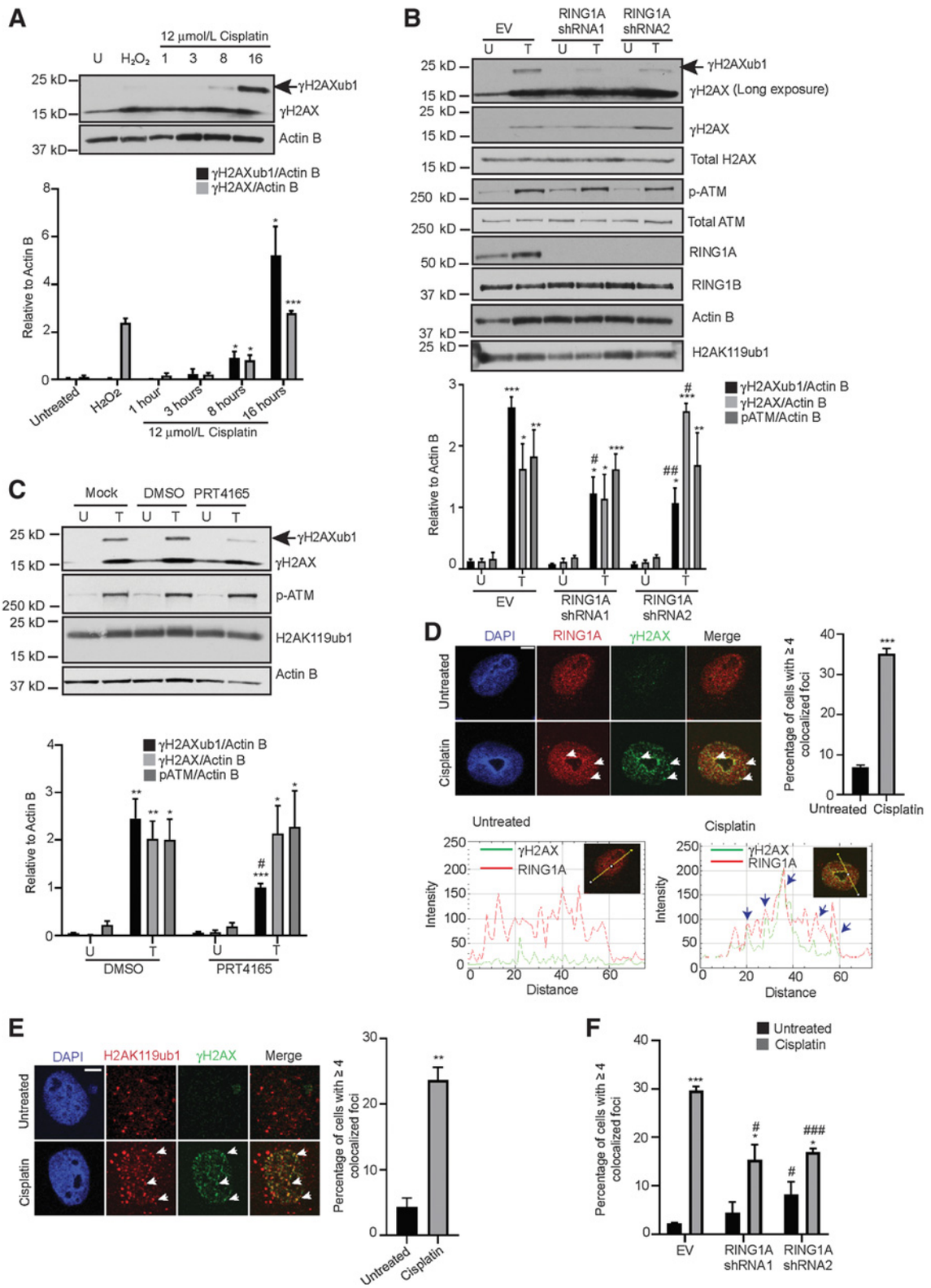

reduction in cisplatin-induced γH2AXub1 after RING1A KD (Supplementary Fig. S1F). Double KD of RING1A and RING1B reduced cisplatin-induced γH2AXub1 to the same extent as RING1A KD alone, suggesting that RING1B does not contribute to the monoubiquitination of γH2AX (Supplementary Fig. S1G). pATM and total ATM protein levels were not altered by RING1A KD plus cisplatin (**Fig. 1B**), and basal H2AK119ub1 or RING1B levels were not significantly altered in RING1A KD cells (**Fig. 1B**). RING1A KD also resulted in reduction in carboplatin-induced γH2AXub1 with no change in the levels of γH2AX (Supplementary Fig. S1H).

The E3 ligase inhibitor PRT4165 inhibits BMI1-RING1A–mediated ubiquitination of H2AK119 in a dose- and time-dependent manner and inhibits γH2AXub1 in response to IR-induced DSBs (24). Of the total H2A basally present in cells, 5% to 15% has been shown to be monoubiquitinated due to role of PRC1 in repression of homeobox (Hox) genes and X chromosome inactivation (25, 26). Combined treatment with PRT4165 and cisplatin for 8 hours had no effect on basal H2AK119ub1 levels, though cisplatin-induced γH2AXub1 levels were reduced (**Fig. 1C**). PRT4165 treatment had no effect on cisplatin-induced γH2AX and pATM levels (**Fig. 1C**).

Proteins involved in DDR localize to and accumulate at DNA damage sites forming foci and BMI1 and RING1B form foci at sites of IR, enzyme-induced DSBs, and sites of UV damage (13–15, 27). Therefore, we were interested in examining if PRC1 members form foci at sites of cisplatin-induced DNA damage. Cisplatin treatment increased ($P < 0.001$) the number of cells with colocalization of RING1A and γH2AX foci (**Fig. 1D**) demonstrating that RING1A is present at sites of DNA damage. RGB profiling of untreated and cisplatin-treated cells demonstrated RING1A colocalization with γH2AX (**Fig. 1D**), confirming the colocalization. Even though BMI1 KD had no effect on cisplatin-induced γH2AXub1 (Supplementary Fig. S1D), BMI1 did form foci and localized to sites of platinum-induced DNA damage (Supplementary Fig. S1I).

The role of RING1A in γH2AXub1 induction suggested lysine 119 as the site of monoubiquitination. However, an antibody against total H2AK119ub1 was unable to detect cisplatin-induced changes in H2Aub1 by Western blot, likely because the basal PRC1-mediated H2AK119ub1 masks platinum-induced changes (in contrast, as shown in **Fig. 1C**, the γH2AX antibody specifically detected cisplatin damage-induced γH2AX and γH2AXub1). Alternatively, using immunofluorescence, we observed that cisplatin treatment resulted in an increase in the percentage of cells with H2AK119ub1 at DNA damage foci (**Fig. 1E**). A representative RGB profile of a cisplatin-treated cell further confirmed colocalization (Supplementary Fig. S2A). Treatment of RING1A KD cells with cisplatin reduced the percentage of cells with H2AK119ub1 at the damage foci compared with control, confirming that the platinum-induced monoubiquitination of γH2AX is mediated by RING1A and occurs on K119 (**Fig. 1F**; Supplementary Fig. S2B–S2D). Altogether, these results suggest that RING1A contributes to γH2AX monoubiquitination in response to platinum DNA damage.

Knockdown of GG-NER proteins reduces cisplatin-induced γH2AXub1

Cisplatin primarily induces intrastrand adducts that can be repaired by both modes of the NER pathway (7, 28), global genome NER (GG-NER repairs lesions throughout the genome), and transcription coupled NER (TC-NER repairs lesions recognized by stalling of RNA polymerase II; ref. 29). Xeroderma pigmentosum complementation group C (XPC) is essential for GG-NER and the cockayne syndrome B (CSB) protein is involved in TC-NER (30, 31). XPA has been implicated in early stages of both GG-NER and TC-NER (29, 32). To determine which NER pathway plays a role in cisplatin-induced H2AX monoubiquitination, we knocked down NER pathway components. XPC KD decreased cisplatin-induced γH2AXub1, whereas CSB KD had no effect (**Fig. 2A**; Supplementary Fig. S3A–S3C). XPA KD also reduced cisplatin-induced γH2AXub1 (**Fig. 2B**). Both XPC and XPA KD decreased γH2AX and pATM protein levels (**Fig. 2A** and **B**), albeit these changes were not statistically significant.

We next examined the effect of XPC and XPA KD on RING1A localization to sites of cisplatin DNA damage. Both XPC and XPA KD decreased the percentage of cells showing RING1A localization to DNA damage foci (**Fig. 2C** and **D**; Supplementary Fig. S3D), suggesting that GG-NER contributes to RING1A localization to sites of platinum DNA damage. However, RING1A localization was not completely abrogated by XPC or XPA KD, suggesting that other repair pathways may also contribute to RING1A localization to DNA damage sites.

Inhibition of HRR reduces platinum-induced γH2AXub1

ICLs formed by cisplatin block DNA replication and transcription and are processed by the FA and HRR pathways (7). As expected, treatment of OVCAR5 or Kuramochi cells with the IC_{50} doses of cisplatin resulted in ATM phosphorylation at S1981 (**Fig. 3A**; Supplementary Fig. S1A), and carboplatin also activated pATM in OVCAR5 cells (Supplementary Fig. S1B). Accumulation of H2Aub1 at sites of enzyme-induced DSBs was shown to be dependent on ATM (33), and we hypothesized that ATM inhibition would alter platinum-induced γH2AXub1. Treatment of OVCAR5 cells with ATMi (15 μmol/L KU-55933) followed by 8-hour cisplatin treatment reduced cisplatin-induced γH2AXub1 (**Fig. 3B**). ATMi also reduced

Figure 1.

RING1A mediates platinum-induced monoubiquitination of γH2AX. **A,** OVCAR5 cells were untreated (U) or treated with 12 μmol/L cisplatin (IC_{50} dose) for 1, 3, 8, and 16 hours or with 2 mmol/L H_2O_2 for 30 minutes (used as a negative control). Cell lysates were analyzed by Western blot. Graph depicts mean ± SEM of densitometric analysis of indicated proteins relative to Actin B at the indicated time points ($N = 3$). **B,** OVCAR5 cells infected with EV or 2 different RING1A shRNAs were untreated (U) or treated (T) with 12 μmol/L cisplatin for 8 hours. Data are presented as in **A**. **C,** OVCAR5 cells were either untreated (U) or treated with 12 μmol/L cisplatin (T) alone or in combination with DMSO or 10 μmol/L PRT4165 for 8 hours. Data are presented as in **A**. **D,** OVCAR5 cells were treated with 12 μmol/L cisplatin for 8 hours. Immunofluorescence analysis was performed for RING1A (red) and the damage marker γH2AX (green). Merge image shows overlap of γH2AX and RING1A. White arrows indicate examples of RING1A foci that colocalize with γH2AX. Graph displays mean percentage of cells with ≥ 4 γH2AX and RING1A colocalized foci ± SEM ($N = 3$). Scale bar = 5 μm. A representative RGB profile of untreated and cisplatin treated cell showing RING1A colocalization with γH2AX. Blue arrows point to foci which colocalize. **E,** OVCAR5 cells were treated as in **D**. Immunofluorescence analysis was performed for H2AK119ub1 (Red) and γH2AX (green). Merge image shows overlap of H2AK119ub1 and γH2AX. White arrows indicate examples of H2AK119 foci that colocalize with γH2AX. Graph displays mean percentage of cells with ≥4 γH2AX and H2AK119ub1 colocalized foci ± SEM ($N = 3$). Scale bar = 5 μm. **F,** OVCAR5 cells infected with EV or 2 different RING1A shRNAs were untreated or treated with 12 μmol/L cisplatin for 8 hours and immunofluorescence was performed as in **E**. Graph displays mean percentage of cells with ≥4 γH2AX and H2AK119ub1 colocalized foci ± SEM ($N = 3$). Statistical significance was calculated using Student *t* test. For all U versus T, *P* values * < 0.05, ** <0.005, and *** < 0.0005. For all EV versus RING1A KD or DMSO versus PRT4165, *P* values # < 0.05, ## < 0.005, and ### < 0.0005.

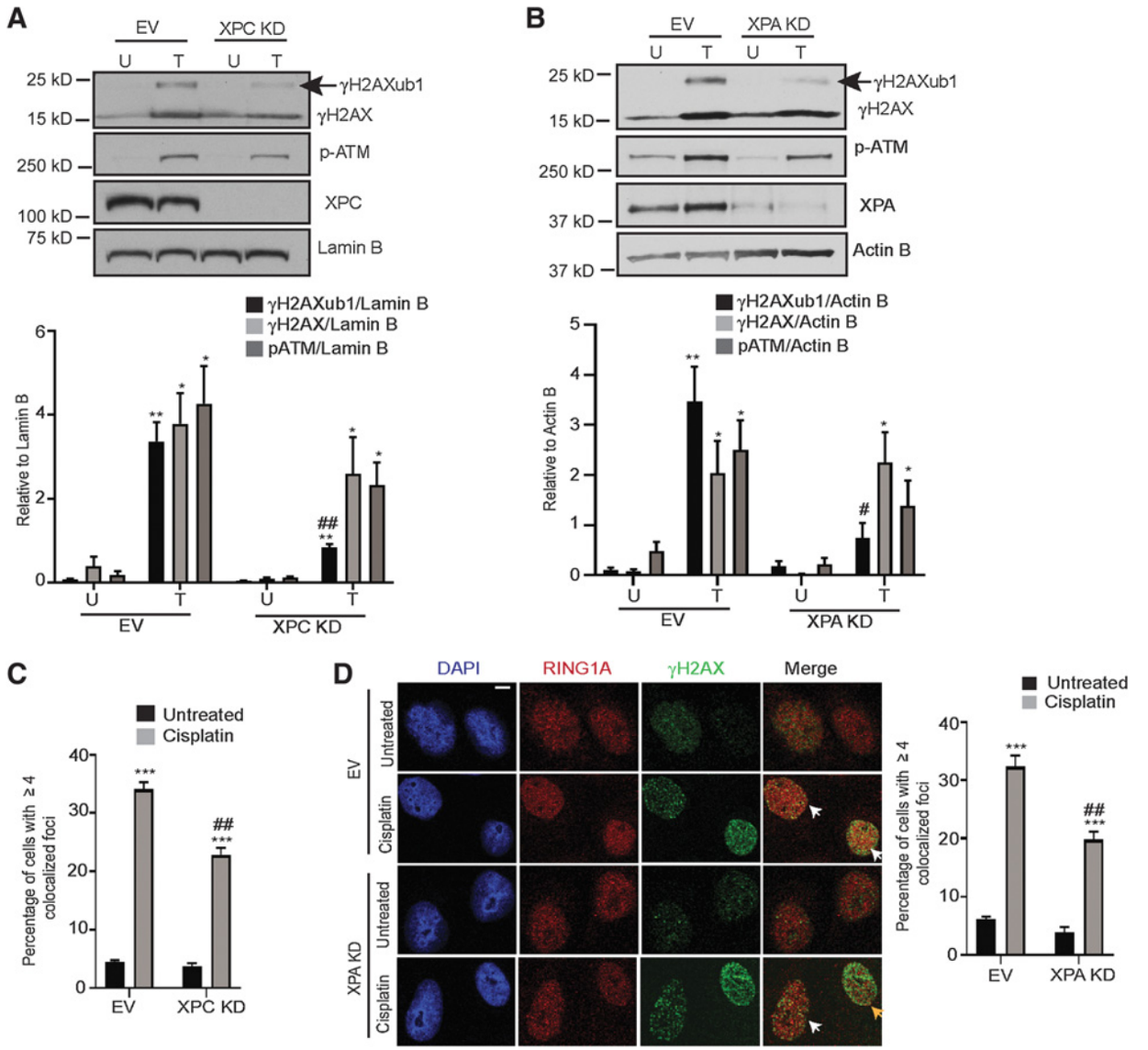

Figure 2.

Knockdown of GG-NER proteins reduces cisplatin-induced γH2AXub1. EV and XPC (**A**) or XPA (**B**) KD OVCAR5 cells were untreated (U) or treated with 12 μmol/L cisplatin for 8 hours (T). Cell lysates were analyzed by Western blot. Graphs depict mean ± SEM of densitometric analysis of indicated proteins relative to indicated housekeeping genes ($N = 3$). **C,** OVCAR5 EV and XPC KD cells were treated with 12 μmol/L cisplatin for 8 hours. Immunofluorescence analysis was performed for RING1A (red) and the damage marker γH2AX (green). Graph depicts mean percentage of cells having ≥ 4 γH2AX and RING1A colocalized foci ± SEM ($N = 3$). **D,** OVCAR5 EV and XPA KD cells were treated and analyzed as in **C**. White arrows indicate examples of cells showing γH2AX and RING1A colocalization, whereas yellow arrows indicate examples of cells which do not have γH2AX and RING1A colocalization (yellow arrow indicates reduction in yellow foci). Scale bar = 5 μm. Statistical significance was calculated using Student *t* test. For all U versus T, *P* values * < 0.05, ** <0.005, and *** < 0.0005. For all EV versus XPC or XPA KD, *P* values # < 0.05, ## < 0.005, and ### < 0.0005.

cisplatin-induced γH2AXub1 in Kuramochi cells and carboplatin-induced γH2AXub1 in OVCAR5 cells (Supplementary Fig. S4A and S4B). Furthermore, treatment with KU-55933 followed by cisplatin reduced RING1A localization to DNA damage foci in comparison with the vehicle control (**Fig. 3C**; Supplementary Fig. S4C). As KD or inhibition of RING1A had no effect on platinum-induced ATM phosphorylation at S1981 or its activation (**Fig. 1B** and **C**), we suggest that RING1A functions downstream of pATM during repair of platinum DNA damage.

An important step in HRR is homology search and strand exchange, catalyzed by Rad51 (34). In response to cisplatin treatment, an expected increase in the percentage of cells having colocalization of Rad51 with γH2AX foci was observed (Supplementary Fig. S4D). Inhibition of Rad51 using B02 followed by cisplatin treatment also reduced γH2AXub1 without altering γH2AX levels (**Fig. 3D**). As a positive control for efficacy of B02 treatment, OVCAR5 cells treated with B02 had a significant reduction in Rad51 foci formation in response to IR (Supplementary Fig. S4E) as previously shown by

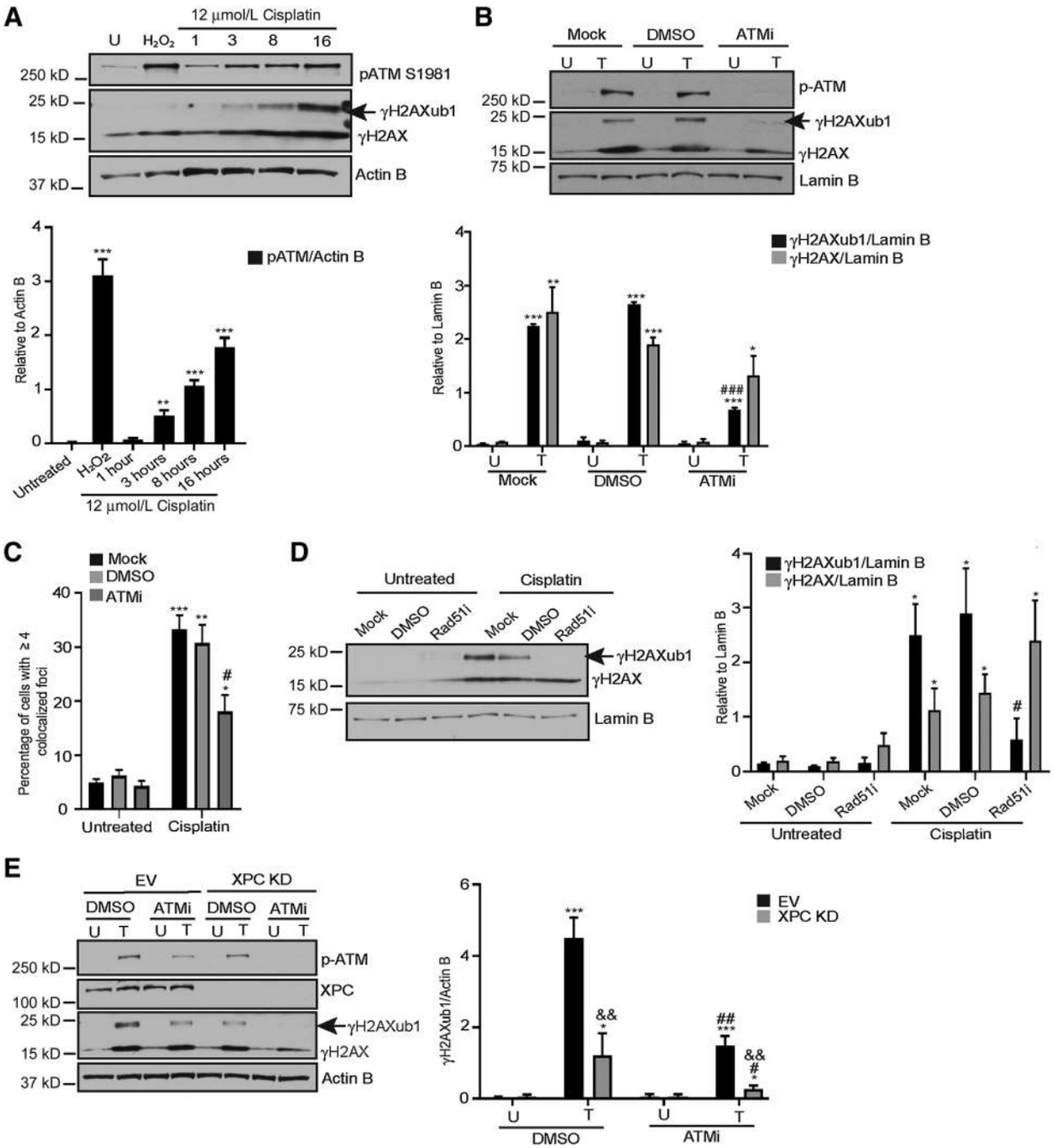

Figure 3.

Inhibition of HRR reduces platinum-induced γH2AXub1. **A,** OVCAR5 cell lysates used in **Fig. 1A** were blotted for pATM. Graphs depict mean ± SEM of densitometric analysis of indicated proteins relative to the indicated housekeeping gene ($N = 3$). **B,** OVCAR5 cells were not pretreated (mock) or pretreated with either DMSO or 15 μmol/L ATM inhibitor (ATMi) Ku-55933 for 1 hour and then untreated (U) or treated (T) with 12 μmol/L cisplatin for 8 hours. Data are presented as in **A**. **C,** OVCAR5 cells were treated as in **B**. Immunofluorescence analysis was performed. Data represent percentage of cells having ≥4 colocalized γH2AX and RING1A foci ± SEM ($N = 3$). **D,** OVCAR5 cells were not pretreated (mock) or pretreated with DMSO or 50 μmol/L Rad51 inhibitor (B02) for 2 hours and then untreated (U) or treated (T) with 12 μmol/L cisplatin for 8 hours. Data are presented as in **A**. **E,** EV or XPC KD OVCAR5 cells were either treated with DMSO or ATM inhibitor (KU-55933) alone (U) or treated (T) with cisplatin for 8 hours. Data are presented as in **A**. Statistical significance was calculated using Student *t* test. For all U versus T, *P* values * < 0.05, ** <0.005, and *** < 0.0005. For all mock or DMSO versus ATMi or Rad51i, *P* values # < 0.05, ## < 0.005, and ### < 0.0005. For EV versus XPC KD in **E**, *P* values & < 0.05, && < 0.005, and &&& < 0.0005.

Huang and colleagues (35). Overall, these results demonstrate that HRR contributes to RING1A localization to sites of DNA damage and platinum-induced γH2AXub1.

Having demonstrated that both GG-NER and HRR contribute to platinum-induced γH2AXub1, we next sought to investigate the combined effect of ATMi and XPC KD on cisplatin-induced γH2AXub1. Cisplatin treatment of EV OVCAR5 cells treated with ATM inhibitor or KD of XPC alone resulted in a reduction in cisplatin-induced γH2AXub1 (**Fig. 3E**), consistent with our previous results (**Figs. 2A** and **3B**). ATMi plus cisplatin treatment further reduced the level of γH2AXub1 in XPC KD cells (**Fig. 3E**). To further confirm that perturbing both NER and HRR pathways simultaneously abrogates cisplatin-induced γH2AXub1, we inhibited Rad51 using B02 in XPC KD cells. As shown previously, Rad51i or XPC KD alone partially reduced cisplatin-induced γH2AXub1, whereas combining Rad51i with XPC KD followed by cisplatin treatment completely abrogated cisplatin-induced γH2AXub1 (Supplementary Fig. S4F). These results suggest that both NER and HRR pathways function in parallel in response to cisplatin DNA damage, and both result in γH2AXub1.

RPA facilitates RING1A localization to sites of cisplatin-induced DNA damage

Based on our data that both GG-NER and HRR pathways result in RING1A-mediated γH2AXub1, we hypothesized that a protein involved in both pathways facilitates RING1A localization to sites of platinum DNA damage. RPA has been implicated as a key player in both GG-NER and DSB repair pathways HRR and nonhomologous end joining (36, 37). The RPA32 subunit of RPA is known to be phosphorylated by ATR and ATM in response to replication stress and IR-induced DSBs regulating downstream protein–protein and protein–DNA interactions (38, 39). RPA32 Serine 33 (S33) is phosphorylated in response to cross-linking agents like UV (37). Cisplatin but not H_2O_2 induced RPA32 phosphorylation at S33 (**Fig. 4A**). Cisplatin treatment increased RPA32 punctate foci which colocalized with the damage marker γH2AX compared with untreated cells (**Fig. 4B**; Supplementary Fig. S5A) as has been demonstrated by others (40). Furthermore, cisplatin treatment increased the percentage of cells with RPA32 foci that colocalized with RING1A in comparison with untreated cells (**Fig. 4C**; Supplementary Fig. S5B).

To test the hypothesis that RPA mediates the localization of RING1A to sites of platinum DNA damage, we pretreated OVCAR5 cells with a reversible RPAi, NERx329, which inhibits RPA binding to ssDNA (41, 42). RPAi reduced cisplatin-induced γH2AXub1 without altering γH2AX levels (**Fig. 4D**). Demonstrating the efficacy of RPAi, OVCAR5 cells pretreated with RPAi prior to UV treatment had a significant reduction in the UV-induced binding of RPA32 to chromatin in comparison with the control (Supplementary Fig. S5C). RPAi also reduced the percentage of cells with colocalization of RING1A and γH2AX foci (**Fig. 4E**; Supplementary Fig. S5D). Altogether, these data suggest that RPA facilitates RING1A localization to sites of cisplatin DNA damage, resulting in γH2AXub1.

RING1A contributes to the repair of cisplatin-induced DNA damage

It was next of interest to investigate the effect of RING1A KD on events downstream of RPA binding to ssDNA, a step which occurs in both GG-NER and HRR pathways (10, 43). RPA binding to ssDNA recruits the ATR-ATRIP complex to damage sites which further results in phosphorylation of RPA32 at S33 and checkpoint kinase 1 (Chk1) at S345, which is required for the activation of G_2–M DNA damage checkpoint (43–46). RING1A KD resulted in reduced platinum-induced phosphorylation of RPA32 at S33 and Chk1 at S345. (**Fig. 5A–C**; validated using a second RING1A shRNA, RING1A shRNA2; Supplementary Fig. S6A). To examine the effect of RING1A KD on the ability of ovarian cancer cells to repair cisplatin DNA damage, we treated OVCAR5 cells with 6 μmol/L cisplatin followed by recovery in platinum-free media. The percentage of cells with γH2AX foci, a measure of the ability of cells to repair DNA damage (20, 47), was maximal at 24 hours of recovery in both EV and RING1A KD cells (**Fig. 5D** and **E**). At 72 hours of recovery, the percentage of γH2AX-positive cells observed in EV cells decreased to approximately 38% relative to the 48-hour time point, suggesting repair of the DNA damage. In contrast, the percentage of RING1A KD cells with γH2AX foci was unchanged at 72 and 96 hours after recovery, with approximately 65% and 62% RING1A KD cells having persistent γH2AX foci, respectively (**Fig. 5D** and **E**; validated by using RING1A shRNA2; Supplementary Fig. S6B). To further examine if RING1A deficiency impairs the ability of cells to survive platinum-induced DNA damage, we treated OVCAR5 cells infected with EV or RING1A shRNA1 or shRNA2 with 6 μmol/L cisplatin for 3 hours followed by recovery in platinum-free media. Cell viability following cisplatin treatment was reduced in RING1A-deficient cells compared with EV cells (**Fig. 5F**). These results suggest that RING1A plays an important role in the repair of platinum-induced DNA damage and knockdown of RING1A increases sensitivity of ovarian cancer cells to platinum.

Discussion

Aberrant DNA damage signaling and repair are prominent features of ovarian tumorigenesis and platinum resistance (48). Furthermore, chromatin modifiers are also dysregulated in ovarian cancer and have been targeted to improve response to chemotherapy agents. Although chromatin modifications have been implicated in the DDR to several types of DNA-damaging agents, their role in the repair of DNA damage caused by platinum-based chemotherapy agents has not been well-studied. Here, we demonstrate for the first time a role for the PRC1 member RING1A and monoubiquitination of γH2AX in the DDR to platinum-induced DNA damage in HGSOC.

Platinum agents are a treatment mainstay for ovarian cancer. DNA damage induced by platinum agents is repaired by NER, FA, and HRR pathways (7, 49, 50). Here, we have implicated both GG-NER and HRR pathways in localization of RING1A to sites of platinum DNA damage and the subsequent increase in γH2AXub1 (Supplementary Fig. S6C). We speculate that platinum-induced γH2AXub1 occurs due to double and ssDNA break intermediates, which are generated during the processing of cisplatin intra- and interstrand cross-links (Supplementary Fig. S6C). The involvement of multiple repair pathways in facilitating RING1A-mediated repair of platinum adducts supports the idea that anticancer therapies targeting multiple DNA repair hubs should be exploited in ovarian cancer and other cancer types as suggested by Deitlein and colleagues (51).

Exhaustion of RPA (a common player in both GG-NER and HRR) during replication stress is demonstrated to be a vital determinant of cisplatin resistance in HGSOC cells (52). We demonstrate that RPA mediates RING1A localization to damage sites connecting NER and HRR pathways to RING1A-mediated γH2AXub1 (Supplementary Fig. S6C). Our findings are consistent with the idea that RPA can orchestrate the localization of many proteins to sites of DNA damage to promote repair (53, 54). Future work is needed to further understand the mechanism that connects RING1A to RPA. RPA plays a vital role in DNA replication and other DNA repair pathways in addition to NER and HRR. The RPAi used in this study blocks the binding of

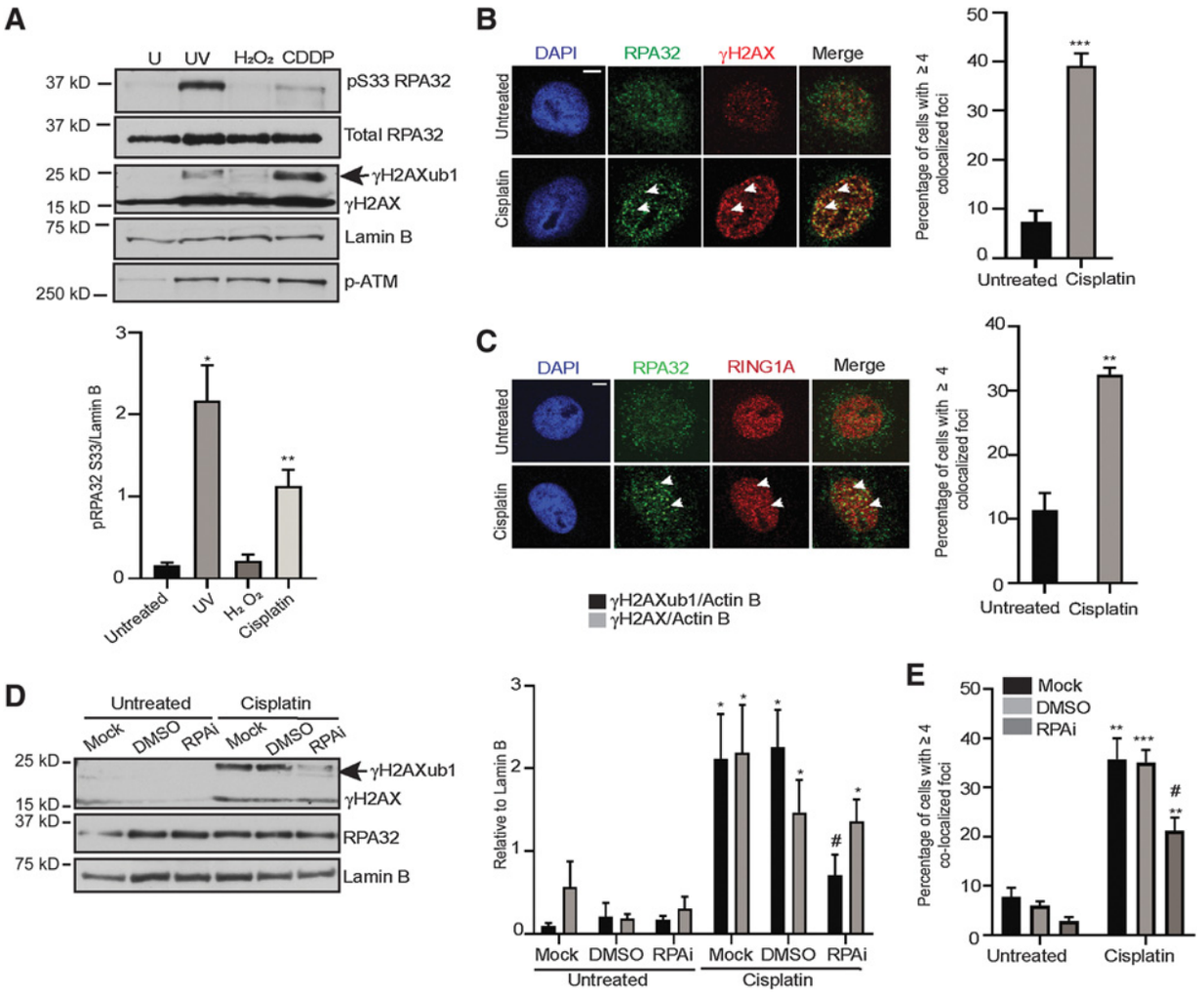

Figure 4.

RPA facilitates RING1A localization to sites of cisplatin-induced DNA damage. **A,** OVCAR5 cells were untreated (U) or treated with 200 mJ/cm^2 UV (positive control) followed by 15-minute recovery, 2 mmol/L H_2O_2 for 30 minutes, or 12 μmol/L cisplatin (CDDP) for 8 hours. H_2O_2 and UV were negative and positive controls, respectively, for pS33 RPA32 phosphorylation. Graphs depict mean ± SEM densitometric analysis of indicated proteins relative to the indicated housekeeping gene ($N = 3$). **B** and **C,** OVCAR5 cells were treated with 12 μmol/L cisplatin for 8 hours, followed by immunofluorescence analysis for indicated antibodies. Graph depicts mean ± SEM percentage of cells with ≥4 RPA32 and γH2AX (**B**), and RPA32 and RING1A (**C**) colocalized foci of $N = 3$ biological replicates. White arrows indicated examples of γH2AX and RING1A foci which colocalize. Scale bar = 5 μm. **D,** OVCAR5 cells were not pretreated (Mock) or pretreated with DMSO or 8 μmol/L NERx329 (RPAi) for 2 hours followed by 8 hours of cisplatin treatment. Data are presented as in **A**. **E,** OVCAR5 cells were not pretreated (Mock) or pretreated with DMSO or 8 μmol/L RPAi for 2 hours and then untreated or treated with cisplatin for 8 hours. Immunofluorescence was performed and analyzed as in **B**. Statistical significance was calculated using Student *t* test. For all U versus T, *P* values * < 0.05, ** <0.005, *** < 0.0005, and ns, not significant. For all mock or DMSO versus RPAi, *P* values # < 0.05, ## < 0.005, and ### < 0.0005.

RPA's OB folds to DNA (42). An inhibitor targeting RPA–DNA interaction such as NERx329 has advantages over other types of RPAis because it inhibits RPA independent from its phosphorylation status. Developing RPAis like NERx329 to be used in combination with platinum could be beneficial in killing rapidly proliferating cancer cells and repair proficient chemoresistant ovarian cancer cells.

Recurrent ovarian tumors have high expression of PRC1 members—BMI1, RING1A, and RING1B (23). We demonstrate that RING1A contributes to platinum-induced monoubiuquitination of γH2AX. Because of limitations of commercially available H2AK119ub antibodies, we detected ubiquitination using an antibody against γH2AX. Our data suggest that cisplatin-induced monoubiquitination of H2AX occurs after its phosphorylation. Although we focused on RING1A-mediated γH2AXub1, monoubiquitination is also likely occurring on H2A in response to platinum. It is possible that sites where damage occurred already contained monoubiquinated H2AX. However, we do not believe this is the case as phosphorylation of H2AX is also induced by H_2O_2 without detection of monoubiquitinated γH2AX (see **Figs. 1A** and **3A**). The persistence of γH2AX foci in RING1A KD cells indicates that RING1A promotes the repair of platinum DNA damage. The increased sensitivity of RING1A KD cells to platinum treatment further confirms that RING1A promotes DNA repair and survival after platinum-induced DNA damage. Although RING1A

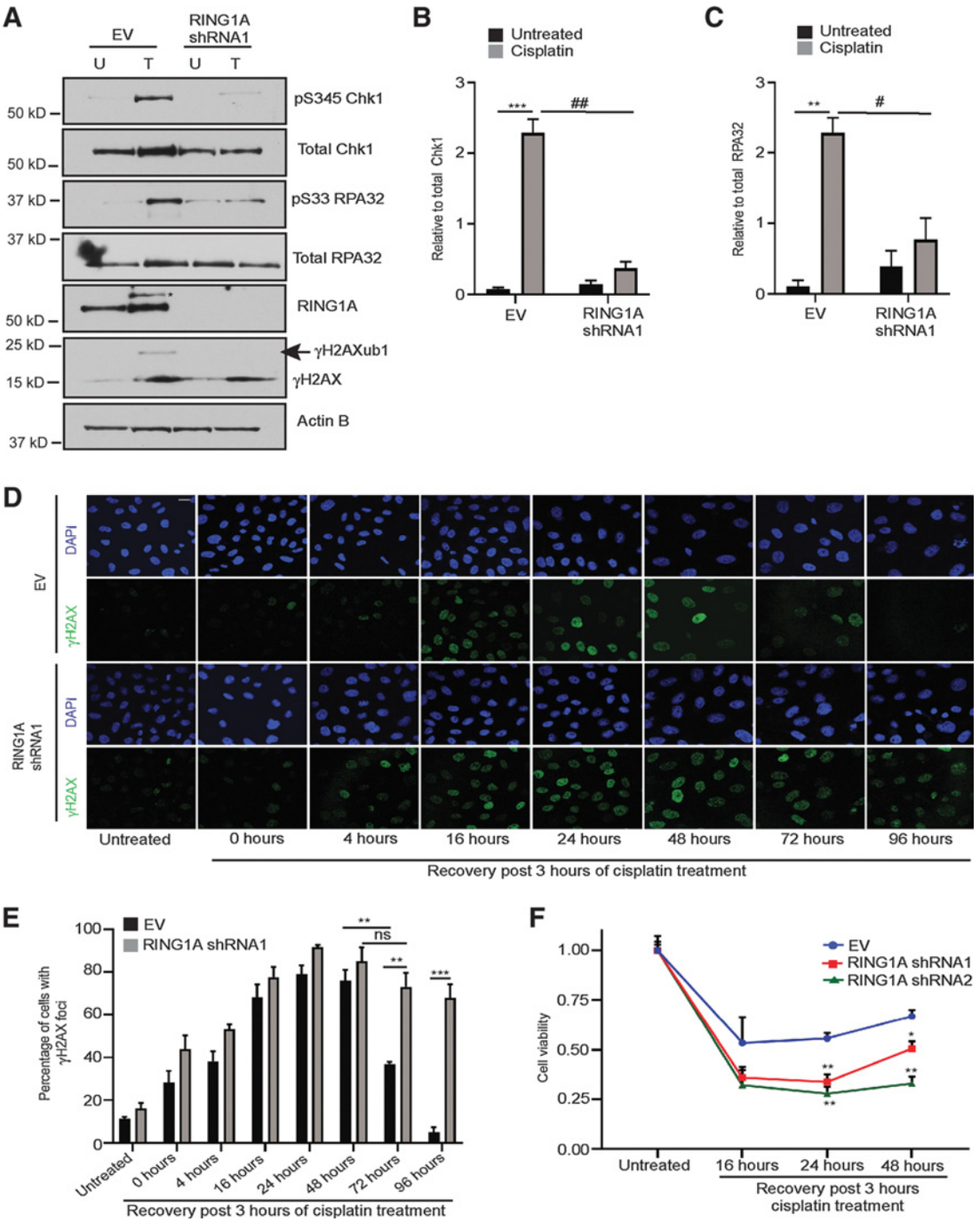

Figure 5.

RING1A contributes to the repair of cisplatin-induced DNA damage. **A,** OVCAR5 cells infected with EV or RING1A shRNA1 were untreated (U) or treated with 12 μmol/L cisplatin for 8 hours. Cell lysates were analyzed by Western blot.* denotes nonspecific band. Graph depicts mean ± SEM of densitometric analysis of $N = 3$ biological replicates of pS345 Chk1 relative to total Chk1 (**B**) and pS33 RPA32 relative to total RPA32 (**C**). For all U versus T, P values ** <0.005, *** < 0.0005, and ns, not significant. For all EV versus RING1A KD, P values # < 0.05, ## < 0.005, and ### < 0.0005. **D,** EV or RING1A KD OVCAR5 cells were treated with 6 μmol/L cisplatin for 3 hours. Cells were then allowed to recover in platinum-free media for the indicated time points followed by immunofluorescence for γH2AX (green) as a surrogate for DNA damage. Representative images of OVCAR5 EV and RING1A KD cells at the indicated time points are displayed. Scale bar = 20 μm. **E,** Graph depicts mean percentage of cells with γH2AX foci ± SEM in $N = 3$ biological replicates. For all EV versus RING1A KD, P values ** <0.005, *** < 0.0005, and ns, not significant. **F,** EV or RING1A KD cells were treated with 6 μmol/L cisplatin for 3 hours. Cells were then allowed to recover in platinum-free media for the indicated time points. Graph depicts mean cell viability ± SEM in $N = 3$ biological replicates of cells after recovery in platinum-free media relative to respective untreated cells. For all EV versus RING1A KD, P values * < 0.05 and ** <0.005.

KD may alter chromatin dynamics and hence indirectly result in persistent γH2AX foci, the alteration of the G_2–M checkpoint suggests that RING1A KD alters the DDR. Together, our data demonstrate that RING1A plays an important role in repair of cisplatin-induced DNA damage in ovarian cancer cells.

PRC1 complexes are heterogeneous in nature and can contain several different E3 ligases (55). In our study, BMI1 localized to sites of platinum DNA damage (Supplementary Fig. S1I); however, KD of BMI1 or RING1B did not affect platinum-induced γH2AXub1 and the presence of RING1B did not compensate for the depletion of RING1A in regard to platinum-induced γH2AXub1 (Supplementary Fig. S1D and S1E). We reason that as there are multiple PRC1 and PRC1-like complexes, and RING1A and RING1B can replace each other, it is likely that a PRC1 or PRC1-like complex having predominantly RING1A as the E3 ligase is involved in the DDR to platinum agents in ovarian cancer cells. Further studies are essential to determine which PRC1 or PRC1-like complex members in addition to RING1A are involved in DDR to platinum agents in other cancer types and why specifically RING1A but not RING1B is involved in DDR of platinum lesions in ovarian cancer cells.

The main obstacle in the use of platinum agents for treatment of ovarian cancer and other cancers like colon and lung is the development of chemotherapy resistance. Our study has furthered our understanding of the role of RING1A in the DDR to platinum agents in ovarian cancer and has established a link between repair pathways and localization of RING1A to damage sites. Collectively, our data support additional preclinical and clinical investigations that will be aimed at investigating the role of RING1A in primary cell lines derived from clinical samples and *in vivo* models of ovarian cancer, increasing the translational impact of targeting RPA and/or RING1A in combination with platinum. RPAis, like the one used in our study, have shown efficacy in regressing the growth of tumors in a xenograft model of non–small cell lung carcinoma (41). Evaluating the effect of such inhibitors in *in vivo* models of ovarian cancer will aid in improving response of patients with recurrent ovarian cancer to standard chemotherapy regimens. Furthermore, our data demonstrate that RING1A KD sensitizes HGSOC cells to platinum. This warrants the need for further development of targeted RING1A inhibitors that can be used *in vivo*, which will potentially aid in preventing the development of platinum resistance. As platinum-based agents are used in chemotherapy regimens in several other cancers, our findings warrant further investigation of the role of PRC1 in the repair of platinum lesions in other cancer types as well.

Disclosure of Potential Conflicts of Interest

J.J. Turchi reports grants from NIH and grants from NERx Biosciences during the conduct of the study; grants and personal fees from NERx Biosciences outside the submitted work; in addition, Dr. Turchi has a patent for RPA inhibitors pending, issued, and licensed to NERx Biosciences. No potential conflicts of interest were disclosed by the other authors.

Authors' Contributions

S. Sriramkumar: Conceptualization, formal analysis, supervision, validation, investigation, visualization, methodology, writing-original draft, writing-review and editing. **T.D. Matthews:** Validation, investigation. **A.H. Ghobashi:** Validation, investigation. **S.A. Miller:** Formal analysis, investigation, visualization. **P.S. VanderVere-Carozza:** Resources, methodology, writing-review and editing. **K.S. Pawelczak:** Resources, methodology. **K.P. Nephew:** Resources, funding acquisition, methodology, writing-review and editing. **J.J. Turchi:** Resources, supervision, methodology, writing-review and editing. **H.M. O'Hagan:** Conceptualization, resources, supervision, funding acquisition, methodology, project administration, writing-review and editing.

Acknowledgments

S. Sriramkumar dedicates this work in the loving memory of her mother Brinda Sriramkumar. This research was funded by Ovarian Cancer Research Alliance grant number 458788 to H.M. O'Hagan and K.P. Nephew. S. Sriramkumar was supported by the Doane and Eunice Dahl Wright Fellowship generously provided by Imogen Dahl. T.D. Matthews was supported by funding provided by Van Andel Institute through the Van Andel Institute - Stand Up To Cancer Epigenetics Dream Team. Stand Up To Cancer is a division of the Entertainment Industry Foundation, administered by AACR. We thank the Indiana University Light Microscopy Imaging Center for their assistance.

The costs of publication of this article were defrayed in part by the payment of page charges. This article must therefore be hereby marked *advertisement* in accordance with 18 U.S.C. Section 1734 solely to indicate this fact.

Received May 3, 2020; revised July 10, 2020; accepted August 6, 2020; published first August 14, 2020.

References

1. Torre LA, Trabert B, DeSantis CE, Miller KD, Samimi G, Runowicz CD, et al. Ovarian cancer statistics, 2018. CA Cancer J Clin 2018;68:284–96.
2. Ozols RF. Treatment goals in ovarian cancer. Int J Gynecol Cancer 2005;15 (Suppl 1):3–11.
3. Vaughan S, Coward JI, Bast RC Jr, Berchuck A, Berek JS, Brenton JD, et al. Rethinking ovarian cancer: recommendations for improving outcomes. Nat Rev Cancer 2011;11:719–25.
4. Stewart DJ. Mechanisms of resistance to cisplatin and carboplatin. Crit Rev Oncol Hematol 2007;63:12–31.
5. Matei D, Nephew KP. Epigenetic attire in ovarian cancer: the emperor's new clothes. Cancer Res 2020;80:3775–85.
6. Dasari S, Tchounwou PB. Cisplatin in cancer therapy: molecular mechanisms of action. Eur J Pharmacol 2014;740:364–78.
7. Kartalou M, Essigmann JM. Mechanisms of resistance to cisplatin. Mutat Res 2001;478:23–43.
8. Kim H, D'Andrea AD. Regulation of DNA cross-link repair by the Fanconi anemia/BRCA pathway. Genes Dev 2012;26:1393–408.
9. Bakkenist CJ, Kastan MB. DNA damage activates ATM through intermolecular autophosphorylation and dimer dissociation. Nature 2003;421:499–506.
10. Marechal A, Zou L. DNA damage sensing by the ATM and ATR kinases. Cold Spring Harb Perspect Biol 2013;5:a012716.
11. Green CM, Almouzni G. When repair meets chromatin. First in series on chromatin dynamics. EMBO Rep 2002;3:28–33.
12. Buchwald G, van der Stoop P, Weichenrieder O, Perrakis A, van Lohuizen M, Sixma TK. Structure and E3-ligase activity of the Ring-Ring complex of polycomb proteins Bmi1 and Ring1b. Embo Journal 2006;25:2465–74.
13. Ismail IH, Andrin C, McDonald D, Hendzel MJ. BMI1-mediated histone ubiquitylation promotes DNA double-strand break repair. J Cell Biol 2010; 191:45–60.
14. Ginjala V, Nacerddine K, Kulkarni A, Oza J, Hill SJ, Yao M, et al. BMI1 is recruited to DNA breaks and contributes to DNA damage-induced H2A ubiquitination and repair. Mol Cell Biol 2011;31:1972–82.
15. Ui A, Nagaura Y, Yasui A. Transcriptional elongation factor ENL phosphorylated by ATM recruits polycomb and switches off transcription for DSB repair. Mol Cell 2015;58:468–82.
16. Bergink S, Salomons FA, Hoogstraten D, Groothuis TA, de Waard H, Wu J, et al. DNA damage triggers nucleotide excision repair-dependent monoubiquitylation of histone H2A. Genes Dev 2006;20:1343–52.
17. Marteijn JA, Bekker-Jensen S, Mailand N, Lans H, Schwertman P, Gourdin AM, et al. Nucleotide excision repair-induced H2A ubiquitination is dependent on MDC1 and RNF8 and reveals a universal DNA damage response. J Cell Biol 2009; 186:835–47.

18. Wang Y, Zong X, Mitra S, Mitra AK, Matei D, Nephew KP. IL-6 mediates platinum-induced enrichment of ovarian cancer stem cells. JCI Insight 2018;3: e122360.
19. Burger K, Schlackow M, Gullerova M. Tyrosine kinase c-Abl couples RNA polymerase II transcription to DNA double-strand breaks. Nucleic Acids Res 2019;47:3467–84.
20. Mah LJ, El-Osta A, Karagiannis TC. gammaH2AX: a sensitive molecular marker of DNA damage and repair. Leukemia 2010;24:679–86.
21. Luczak MW, Zhitkovich A. Monoubiquitinated gamma-H2AX: abundant product and specific biomarker for non-apoptotic DNA double-strand breaks. Toxicol Appl Pharmacol 2018;355:238–46.
22. Hongo A, Seki S, Akiyama K, Kudo T. A comparison of in vitro platinum-DNA adduct formation between carboplatin and cisplatin. Int J Biochem 1994;26: 1009–16.
23. Gui T, Bai H, Zeng J, Zhong Z, Cao D, Cui Q, et al. Tumor heterogeneity in the recurrence of epithelial ovarian cancer demonstrated by polycomb group proteins. Onco Targets Ther 2014;7:1705–16.
24. Ismail IH, McDonald D, Strickfaden H, Xu Z, Hendzel MJ. A small molecule inhibitor of polycomb repressive complex 1 inhibits ubiquitin signaling at DNA double-strand breaks. J Biol Chem 2013;288:26944–54.
25. Cao R, Tsukada Y, Zhang Y. Role of Bmi-1 and Ring1A in H2A ubiquitylation and Hox gene silencing. Mol Cell 2005;20:845–54.
26. de Napoles M, Mermoud JE, Wakao R, Tang YA, Endoh M, Appanah R, et al. Polycomb group proteins Ring1A/B link ubiquitylation of histone H2A to heritable gene silencing and X inactivation. Dev Cell 2004;7:663–76.
27. Rothkamm K, Barnard S, Moquet J, Ellender M, Rana Z, Burdak-Rothkamm S. DNA damage foci: meaning and significance. Environ Mol Mutagen 2015;56: 491–504.
28. Sears CR, Cooney SA, Chin-Sinex H, Mendonca MS, Turchi JJ. DNA damage response (DDR) pathway engagement in cisplatin radiosensitization of non-small cell lung cancer. DNA Repair 2016;40:35–46.
29. de Laat WL, Jaspers NG, Hoeijmakers JH. Molecular mechanism of nucleotide excision repair. Genes Dev 1999;13:768–85.
30. Sugasawa K, Ng JM, Masutani C, Iwai S, van der Spek PJ, Eker AP, et al. Xeroderma pigmentosum group C protein complex is the initiator of global genome nucleotide excision repair. Mol Cell 1998;2:223–32.
31. van den Boom V, Citterio E, Hoogstraten D, Zotter A, Egly JM, van Cappellen WA, et al. DNA damage stabilizes interaction of CSB with the transcription elongation machinery. J Cell Biol 2004;166:27–36.
32. Tanaka K, Miura N, Satokata I, Miyamoto I, Yoshida MC, Satoh Y, et al. Analysis of a human DNA excision repair gene involved in group A xeroderma pigmentosum and containing a zinc-finger domain. Nature 1990;348:73–6.
33. Shanbhag NM, Rafalska-Metcalf IU, Balane-Bolivar C, Janicki SM, Greenberg RA. ATM-dependent chromatin changes silence transcription in cis to DNA double-strand breaks. Cell 2010;141:970–81.
34. Sung P. Catalysis of ATP-dependent homologous DNA pairing and strand exchange by yeast RAD51 protein. Science 1994;265:1241–3.
35. Huang F, Motlekar NA, Burgwin CM, Napper AD, Diamond SL, Mazin AV. Identification of specific inhibitors of human RAD51 recombinase using high-throughput screening. ACS Chem Biol 2011;6:628–35.
36. Jalal S, Earley JN, Turchi JJ. DNA repair: from genome maintenance to biomarker and therapeutic target. Clin Cancer Res 2011;17:6973–84.
37. Binz SK, Sheehan AM, Wold MS. Replication protein A phosphorylation and the cellular response to DNA damage. DNA Repair 2004;3:1015–24.
38. Block WD, Yu Y, Lees-Mille SP. Phosphatidyl inositol 3-kinase-like serine/threonine protein kinases (PIKKs) are required for DNA damage-induced phosphorylation of the 32 kDa subunit of replication protein A at threonine 21. Nucleic Acids Res 2004;32:997–1005.
39. Oakley GG, Patrick SM, Yao J, Carty MP, Turchi JJ, Dixon K. RPA phosphorylation in mitosis alters DNA binding and protein-protein interactions. Biochemistry 2003;42:3255–64.
40. Prasad CB, Prasad SB, Yadav SS, Pandey LK, Singh S, Pradhan S, et al. Olaparib modulates DNA repair efficiency, sensitizes cervical cancer cells to cisplatin and exhibits anti-metastatic property. Sci Rep 2017;7:12876.
41. Mishra AK, Dormi SS, Turchi AM, Woods DS, Turchi JJ. Chemical inhibitor targeting the replication protein A-DNA interaction increases the efficacy of Pt-based chemotherapy in lung and ovarian cancer. Biochem Pharmacol 2015;93: 25–33.
42. Gavande NS, VanderVere-Carozza PS, Pawelczak KS, Vernon TL, Jordan MR, Turchi JJ. Structure-guided optimization of replication protein A (RPA)–DNA interaction inhibitors. ACS Med Chem Lett 2020;11:1118–24.
43. Zou L, Elledge SJ. Sensing DNA damage through ATRIP recognition of RPA-ssDNA complexes. Science 2003;300:1542–48.
44. Ashley AK, Shrivastav M, Nie J, Amerin C, Troksa K, Glanzer JG, et al. DNA-PK phosphorylation of RPA32 Ser4/Ser8 regulates replication stress checkpoint activation, fork restart, homologous recombination and mitotic catastrophe. DNA Repair 2014;21:131–9.
45. Leung-Pineda V, Ryan CE, Piwnica-Worms H. Phosphorylation of Chk1 by ATR is antagonized by a Chk1-regulated protein phosphatase 2A circuit. Mol Cell Biol 2006;26:7529–38.
46. Liu Q, Guntuku S, Cui XS, Matsuoka S, Cortez D, Tamai K, et al. Chk1 is an essential kinase that is regulated by Atr and required for the G(2)/M DNA damage checkpoint. Genes Dev 2000;14:1448–59.
47. Kinner A, Wu W, Staudt C, Iliakis G. Gamma-H2AX in recognition and signaling of DNA double-strand breaks in the context of chromatin. Nucleic Acids Res 2008;36:5678–94.
48. Marsh DJ, Shah JS, Cole AJ. Histones and their modifications in ovarian cancer - drivers of disease and therapeutic targets. Front Oncol 2014;4:144.
49. De Silva IU, McHugh PJ, Clingen PH, Hartley JA. Defining the roles of nucleotide excision repair and recombination in the repair of DNA interstrand cross-links in mammalian cells. Mol Cell Biol 2000;20:7980–90.
50. Hanada K, Budzowska M, Modesti M, Maas A, Wyman C, Essers J, et al. The structure-specific endonuclease Mus81-Eme1 promotes conversion of interstrand DNA crosslinks into double-strands breaks. EMBO J 2006;25: 4921–32.
51. Dietlein F, Thelen L, Reinhardt HC. Cancer-specific defects in DNA repair pathways as targets for personalized therapeutic approaches. Trends Genet 2014; 30:326–39.
52. Belanger F, Fortier E, Dube M, Lemay JF, Buisson R, Masson JY, et al. Replication protein A availability during DNA replication stress is a major determinant of cisplatin resistance in ovarian cancer cells. Cancer Res 2018;78:5561–73.
53. Feeney L, Munoz IM, Lachaud C, Toth R, Appleton PL, Schindler D, et al. RPA-Mediated recruitment of the E3 ligase RFWD3 is vital for interstrand crosslink repair and human health. Mol Cell 2017;66:610–21.
54. Yang Q, Zhu Q, Lu X, Du Y, Cao L, Shen C, et al. G9a coordinates with the RPA complex to promote DNA damage repair and cell survival. Proc Natl Acad Sci U S A 2017;114:E6054–63.
55. Aranda S, Mas G, Di Croce L. Regulation of gene transcription by Polycomb proteins. Sci Adv 2015;1:e1500737.